Construction of high-quality NN potential models

V. G. J. Stoks*
School of Physical Sciences, The Flinders University of South Australia, Bedford Park, South Australia 5042, Australia and Institute for Theoretical Physics, University of Nijmegen, Nijmegen, The Netherlands

R. A. M. Klomp,† C. P. F. Terheggen,† and J. J. de Swart†
Institute for Theoretical Physics, University of Nijmegen, Nijmegen, The Netherlands
(Received 29 September 1993)

We present an updated version (Nijm93) of the Nijmegen soft-core potential, which gives a much better description of the np data than the older version (Nijm78). The χ^2 per datum is 1.87. The configuration-space and momentum-space versions of this potential are exactly equivalent, a unique feature among meson-theoretical potentials. We also present three new NN potential models: a nonlocal Reid-like Nijmegen potential (Nijm I), a local version (Nijm II), and an updated regularized version (Reid93) of the Reid soft-core potential. These three potentials all have a nearly optimal χ^2 per datum and can therefore be considered as alternative partial-wave analyses. All potentials contain the proper charge-dependent one-pion-exchange tail.

PACS number(s): 13.75.Cs, 12.39.Pn, 21.30.+y

I. INTRODUCTION

In the past many nucleon-nucleon (NN) potentials were constructed, which were supposed to fit the NN scattering data available at the time of construction. The older models, from the 1950s and 1960s, are no longer suitable for describing the present set of more numerous and much more accurate data without refitting the parameters. Out of the various potential models constructed in the 1970s, the better ones fitted the data with $\chi^2/N_{\rm data}$ of about 2, where $N_{\rm data}$ denotes the number of NN scattering data available at that time in the 0–350 MeV energy range. The potentials constructed in the 1980s have only slightly improved on this in the sense that, although they have been fitted to try to describe the newer and much more accurate data, these models still have $\chi^2/N_{\rm data} \approx 2$. This number should be compared with $\chi^2_{\rm min}/N_{\rm data} = 0.99$, obtained in the recently finished Nijmegen NN multienergy partial-wave analysis [1] (PWA93) of all pp and np scattering data below 350 MeV. On statistical grounds, $\chi^2_{\rm min}/N_{\rm data} \approx 1$ is about the best one can expect to get in partial-wave analyses or for potential models.

In a recent paper [2], we investigated the quality with respect to the pp scattering data below 350 MeV of a number of NN potentials that had appeared in the literature. We found that only a few of the potential models we investigated are of a satisfactory quality. These models are the Reid soft-core potential [3] Reid68, the Nijmegen soft-core potential [4] Nijm78, and the new Bonn pp potential [5] Bonn89. The latter is a readjustment of the momentum-space full Bonn potential [6], in order to fit the pp data. If we do not consider the very low-energy (0–2 MeV) pp data, also the parametrized Paris potential [7] Paris80 gives a satisfactory description of the data. The results of Ref. [2] indicate that, at present, the best potential models have $\chi^2/N_{pp} \gtrsim 1.9$, where N_{pp} denotes the number of pp scattering data. Moreover, only models which have explicitly included the pp data in their fit belong to this category. Potential models which have been fitted only to the np data often give a poor description of the pp data, even after applying the necessary corrections for the Coulomb interaction. In Ref. [2] we have demonstrated that most np potentials unfortunately do not automatically fit the pp data, a fact which has been generally overlooked. Any NN potential should be fitted to the pp data as well as to the np data in order to be able to describe all NN scattering data.

Over the last decade the quality of the np data has increased considerably. Consequently, the older potentials (Reid68, Nijm78, Paris80) do not fit these data very well. Also, the much newer Bonn potentials already needed revisions and updates [5,8]. In this paper we present updates of the Nijm78 and Reid68 potentials, denoted by Nijm93 and Reid93, respectively. Because our analysis of the np data (and hence our careful scrutiny of the np data) has only recently been finished [1], we originally constructed an update (Nijm92pp) of the Nijm78 potential for the pp data only. This pp potential was used in our earlier preliminary np analyses [9–11] to parametrize the isovector partial waves. It has $\chi^2/N_{pp} = 1.4$, which is not as good as the Nijmegen PWA93. One can wonder whether it is at all possible to construct a new class of potential models which fit the NN data with the almost perfect $\chi^2/N_{\rm data} \approx 1$. The answer turns out to be affirmative. This could already be surmised from the Nijmegen PWA93, because this analysis is in essence an energy-dependent potential fitted to the scattering

*Permanent address: School of Physical Sciences, The Flinders University of South Australia, Bedford Park, South Australia 5042, Australia.
†Electronic address: thefalg@sci.kun.nl

data. (The reason for us using an energy-dependent potential is nothing more than just convenience.) In the partial-wave analysis we need 39 parameters to reach $\chi^2/N_{\rm data} = 0.99$, whereas a conventional potential model typically has only 10–15 free parameters. It is therefore perhaps not surprising that the 15-parameter update (Nijm93) of the Nijm78 potential, which fits the *NN* data with $\chi^2/N_{\rm data} = 1.87$, cannot compete in quality with the Nijmegen PWA93. To obtain a high-quality potential we decided some years ago to follow a different approach.

Because the Nijm92*pp* potential already gives a reasonable description of the *pp* data, this model forms the basis for the construction of a high-quality potential, which *can* compete with the Nijmegen PWA93. We adjust in each partial wave separately only a few of the parameters of this potential [12]. This way we will be able to construct a potential model which fits the data with $\chi^2/N_{\rm data} \approx 1$. The resulting Reid-like potential Nijm I gives a very good fit to the data with $\chi^2/N_{\rm data} = 1.03$.

The Nijm I potential contains momentum-dependent terms (as do the Nijm78 and Nijm93 potentials), which in configuration space give rise to a nonlocal structure $[\Delta\varphi(r) + \varphi(r)\Delta]$ to the potential. We also constructed a purely local Nijm II potential, where these momentum-dependent terms were intentionally omitted. This local potential Nijm II gives an equally good fit to the data as the nonlocal potential Nijm I. Finally, we constructed a regularized update of the Reid68 potential [3], called Reid93. This Reid93 model is also a local potential and fits the scattering data very well. These latter three potential models are in a sense also alternative partial-wave analyses, because they have roughly the same number of fit parameters as our Nijmegen PWA93, these parameters were fitted to the same database, and the potential models achieve nearly the same values of $\chi^2_{\rm min}$ as the Nijmegen PWA93 (i.e., close to the expectation value). Hence, the differences between, e.g., the phase parameters of these models provide an indication for the systematic error in the Nijmegen partial-wave analyses.

In Sec. II we briefly discuss some general features of *NN* potentials. In Sec. III we give more details regarding the explicit form of the potentials used in this work. Two of these potentials are based on the original Nijm78 potential, whereas the third is a regularized update of the Reid68 potential in the sense that also in this new model each partial wave is parametrized by a number of Yukawa functions. In Sec. IV we discuss the fitting procedure and the potentials are presented in more detail.

II. GENERAL OUTLINE

The *NN* potential can be described in momentum space and in configuration space. Since it is difficult to solve the full four-dimensional scattering equation, it has become common practice first to make a reduction to a three-dimensional scattering equation. Various choices are possible, and it is important to note that the potential derived within the chosen reduction scheme should *only* be used in the scattering equation corresponding to that particular reduction scheme. These three-dimensional scattering equations can always be written in the form of the momentum-space version of the Lippmann-Schwinger equation. If the kinematics is treated relativistically, this is called the relativistic Lippmann-Schwinger equation. In configuration space, the differential form of this integral equation is the Schrödinger equation.

The configuration-space potentials are to be used either in the nonrelativistic or the relativistic Schrödinger equation:

$$(\Delta + k^2)\psi = 2M_r V \psi \ , \tag{1}$$

where Δ is the Laplacian, and where (non)relativistic refers to the kinematics. For nonrelativistic kinematics the relation between the center-of-mass energy E and the center-of-mass momentum squared k^2 reads $E = k^2/2M_r$, whereas for relativistic kinematics it reads $E = \sqrt{k^2 + M_1^2} + \sqrt{k^2 + M_2^2} - M_1 - M_2$.

The earliest potential models were configuration-space potentials to be used in the nonrelativistic Schrödinger equation. They were phenomenological or semiphenomenological parametrizations, based on a general form for the potential. The potential must be invariant under rotations, reflections, and time reversal, and can be written [13] as the sum of six independent terms, $V = \sum_{i=1}^{6} V_i P_i$. A common choice for the six operators P_i in configuration space is

$$\begin{aligned} P_1 &= 1, \\ P_2 &= \boldsymbol{\sigma}_1 \cdot \boldsymbol{\sigma}_2, \\ P_3 &= S_{12} = 3(\boldsymbol{\sigma}_1 \cdot \hat{\mathbf{r}})(\boldsymbol{\sigma}_2 \cdot \hat{\mathbf{r}}) - (\boldsymbol{\sigma}_1 \cdot \boldsymbol{\sigma}_2), \\ P_4 &= \mathbf{L} \cdot \mathbf{S}, \\ P_5 &= Q_{12} = \tfrac{1}{2}[(\boldsymbol{\sigma}_1 \cdot \mathbf{L})(\boldsymbol{\sigma}_2 \cdot \mathbf{L}) + (\boldsymbol{\sigma}_2 \cdot \mathbf{L})(\boldsymbol{\sigma}_1 \cdot \mathbf{L})], \\ P_6 &= \tfrac{1}{2}(\boldsymbol{\sigma}_1 - \boldsymbol{\sigma}_2) \cdot \mathbf{L}. \end{aligned} \tag{2}$$

These operators are also frequently referred to as the central, spin-spin, tensor, spin-orbit, quadratic spin-orbit, and antisymmetric spin-orbit operators, respectively. For identical-particle scattering, the antisymmetric spin-orbit operator P_6 cannot contribute, whereas V_6 vanishes when charge independence is assumed (which is usually the case for *NN* potential models). In general [13], each potential form V_i in configuration space is a function of r^2, and of the operators p^2 and L^2. In most approaches one only keeps the dependence on r^2, while the p^2 dependence (when included) is often only present in a linear way in the central potential V_1. The inclusion of the Q_{12} operator was found to be necessary, because otherwise it was impossible to describe simultaneously the $^1S_0$ and $^1D_2$ phase shifts using the same static potential. The presence of the operator Q_{12} in the potential can to a certain extent be simulated by introducing nonlocal potentials [14].

In the expansion $\sum_{i=1}^{6} V_i P_i$, the potential forms V_i are generally assumed to be the same in all partial waves. The potential differences between the partial waves are dictated by the differences in the expectation values of

the operators P_i in these partial waves. The Reid68 potential [3], however, is based on a quite different approach. Rather than having six potential forms V_i which are the same for all partial waves, now each partial wave is parametrized separately. The potential forms V_i therefore not only depend on r^2 and L^2, but also on S^2 and J^2. In this paper we present some potentials based on this approach that each partial wave is parametrized independently. We refer to these models as Reid-like models.

With the discovery of the heavy mesons in the 1960s, it became common practice to write the potential as a sum over one-boson-exchange (OBE) potentials. The expressions for these OBE potentials are usually derived in momentum space. Introducing momentum vectors

$$\mathbf{k} = \mathbf{p}_f - \mathbf{p}_i, \quad \mathbf{q} = \tfrac{1}{2}(\mathbf{p}_f + \mathbf{p}_i), \quad \mathbf{n} = \mathbf{q} \times \mathbf{k} \ ,$$

in terms of initial ($\mathbf{p}_i$) and final ($\mathbf{p}_f$) momenta, the equivalent in momentum space to Eq. (2) reads

$$\begin{aligned} P_1 &= 1 \ , \\ P_2 &= \boldsymbol{\sigma}_1 \cdot \boldsymbol{\sigma}_2 , \\ P_3 &= (\boldsymbol{\sigma}_1 \cdot \mathbf{k})(\boldsymbol{\sigma}_2 \cdot \mathbf{k}) - \frac{1}{3}\mathbf{k}^2(\boldsymbol{\sigma}_1 \cdot \boldsymbol{\sigma}_2) , \\ P_4 &= \frac{i}{2}(\boldsymbol{\sigma}_1 + \boldsymbol{\sigma}_2) \cdot \mathbf{n} , \\ P_5 &= (\boldsymbol{\sigma}_1 \cdot \mathbf{n})(\boldsymbol{\sigma}_2 \cdot \mathbf{n}) , \\ P_6 &= \frac{i}{2}(\boldsymbol{\sigma}_1 - \boldsymbol{\sigma}_2) \cdot \mathbf{n} . \end{aligned} \tag{3}$$

The potential forms V_i in momentum space are functions of $\mathbf{k}$, $\mathbf{q}$, $\mathbf{n}$, and the energy. Although Eq. (3) provides an adequate set of six linearly independent operators, the Q_{12} operator in configuration space is *not* the exact Fourier transform of the $(\boldsymbol{\sigma}_1 \cdot \mathbf{n})(\boldsymbol{\sigma}_2 \cdot \mathbf{n})$ operator in momentum space. This is of importance if we want both the momentum-space and the configuration-space versions to produce exactly the same phase shifts and bound states, which is only possible when the configuration-space version is the exact Fourier transform of the momentum-space version, and vice versa. This implies [15] that we have to use the inverse Fourier transform of the Q_{12} operator; i.e., the potential contribution $(\boldsymbol{\sigma}_1 \cdot \mathbf{n})(\boldsymbol{\sigma}_2 \cdot \mathbf{n})\, V_5(\mathbf{k}^2)$ is to be replaced by

$$P_5 V_5(\mathbf{k}^2) - P_5' \int_{\infty}^{\mathbf{k}^2} d\mathbf{k}'^2 V_5(\mathbf{k}'^2) \ , \tag{4}$$

where

$$\begin{aligned} P_5' = {} & [(\boldsymbol{\sigma}_1 \cdot \mathbf{q})(\boldsymbol{\sigma}_2 \cdot \mathbf{q}) - \mathbf{q}^2(\boldsymbol{\sigma}_1 \cdot \boldsymbol{\sigma}_2)] \\ & - \tfrac{1}{4}[(\boldsymbol{\sigma}_1 \cdot \mathbf{k})(\boldsymbol{\sigma}_2 \cdot \mathbf{k}) - \mathbf{k}^2(\boldsymbol{\sigma}_1 \cdot \boldsymbol{\sigma}_2)] \ . \end{aligned} \tag{5}$$

Other restrictions imposed on the momentum-space potential forms V_i in that case are that they should not depend on the energy, while the $\mathbf{q}$ dependence should be of second order at most (see also below).

When the potentials are evaluated in momentum space and then Fourier transformed to configuration space, they are usually first regularized to remove the singularities at the origin. This can be achieved by introducing a form factor $F(\mathbf{k}^2)$. A typical Fourier transform, encountered in transforming the momentum-space potential to configuration space, then reads

$$\begin{aligned} \int \frac{d^3k}{(2\pi)^3} \frac{e^{i\mathbf{k}\cdot\mathbf{r}}}{\mathbf{k}^2 + m^2} \left(\mathbf{k}^2\right)^n F(\mathbf{k}^2) &\equiv \frac{m}{4\pi}(-m^2)^n \phi_C^n(r) \\ &= \frac{m}{4\pi}(-\boldsymbol{\nabla}^2)^n \phi_C^0(r) \ . \end{aligned} \tag{6}$$

The results for various frequently used choices are the following.

(i) No form factor at all, $F(\mathbf{k}^2) = 1$. This yields the familiar Yukawa function

$$\phi_C^0(r) = e^{-mr}/mr \ , \tag{7}$$

and the singularities at the origin are still present.

(ii) Monopole form factor, $F(\mathbf{k}^2) = (\Lambda^2 - m^2)/(\Lambda^2 + \mathbf{k}^2)$, normalized such that at the pole $F(-m^2) = 1$. This yields

$$\phi_C^0(r) = \left[e^{-mr} - e^{-\Lambda r}\right]/mr \ . \tag{8}$$

(iii) Dipole form factor, $F(\mathbf{k}^2) = (\Lambda^2 - m^2)^2/(\Lambda^2 + \mathbf{k}^2)^2$, yielding

$$\phi_C^0(r) = \left[e^{-mr} - e^{-\Lambda r}\left(1 + \frac{\Lambda^2 - m^2}{2\Lambda^2}\Lambda r\right)\right] \Big/ mr \ . \tag{9}$$

(iv) Exponential form factor, $F(\mathbf{k}^2) = e^{-\mathbf{k}^2/\Lambda^2}$, yielding

$$\begin{aligned} \phi_C^0(r) = e^{m^2/\Lambda^2} \Bigg[& e^{-mr} \mathrm{erfc}\left(\frac{m}{\Lambda} - \frac{\Lambda r}{2}\right) \\ & - e^{mr} \mathrm{erfc}\left(\frac{m}{\Lambda} + \frac{\Lambda r}{2}\right)\Bigg] \Big/ 2mr \ , \end{aligned} \tag{10}$$

where $\mathrm{erfc}(x)$ is the complementary error function

$$\mathrm{erfc}(x) = \frac{2}{\sqrt{\pi}} \int_x^{\infty} dt\, e^{-t^2} \ .$$

We follow the normalization of Ref. [4]. This means that for the exponential form factor $F(0) = 1$.

Because $\mathbf{k}^2$ can be written as $(\mathbf{k}^2 + m^2) - m^2$, we find that in the absence of a form factor

$$\phi_C^1(r) = \phi_C^0(r) - 4\pi\delta^3(m\mathbf{r}) \ . \tag{11}$$

When there is a form factor, this relation still holds, but the δ-function contribution is smeared out.

Using our definition (6), the Fourier transforms for the tensor and spin-orbit potentials can be simply expressed in terms of derivatives of the central function, i.e.,

$$\begin{aligned} \phi_T^0(r) &= \frac{1}{3m^2} r \frac{d}{dr}\left(\frac{1}{r}\frac{d}{dr}\right) \phi_C^0(r) \ , \\ \phi_{\mathrm{SO}}^0(r) &= -\frac{1}{m^2}\frac{1}{r}\frac{d}{dr}\phi_C^0(r) \ . \end{aligned} \tag{12}$$

In order to ensure regularity at the origin for the tensor and spin-orbit functions, one must choose at least the dipole or exponential form factor. In that case, the tensor function also vanishes at the origin, as it should.

The presence of explicit momentum-dependent terms in the momentum-space potential gives rise to nonlocal structures in the potential in configuration space. The $\mathbf{q}^2$ terms pose no difficulties for the configuration-space potential as long as they are linear in $\mathbf{q}^2$. The typical Fourier transform of such a term is given by

$$\int \frac{d^3k}{(2\pi)^3} \frac{e^{i\mathbf{k}\cdot\mathbf{r}}}{\mathbf{k}^2+m^2}\left(\mathbf{q}^2+\tfrac{1}{4}\mathbf{k}^2\right)F(\mathbf{k}^2) = -\frac{m}{4\pi}\left[\Delta\frac{\varphi(r)}{2M_r}+\frac{\varphi(r)}{2M_r}\Delta\right], \quad (13)$$

where $\varphi(r) = M_r\phi_C^0(r)$. It is well known how to handle such a $(\Delta\varphi+\varphi\Delta)$ term [16]. The absence of $\mathbf{q}^2$ terms in the momentum-space potential will result in a radially local configuration-space potential.

The three new potential models (Nijm93, Nijm I, and Nijm II) presented in this paper are based on the original Nijm78 potential with the exponential form factor, whereas the update of the Reid68 potential (Reid93) is regularized using a dipole form factor.

III. STRUCTURE OF THE POTENTIALS

A. One-pion-exchange potential

An important feature of the potential models presented in this paper is that in the one-pion-exchange (OPE) part of the potential, we explicitly distinguish between neutral-pion and charged-pion exchange. The pion masses are [17] $m_{\pi^0} = 134.9739$ MeV and $m_{\pi^\pm} = 139.5675$ MeV. Almost all other potentials that have appeared in the literature use a mean pion mass. In these other models the isovector *np* phase parameters are *larger* in magnitude than the corresponding *pp* phase parameters. By explicitly including the pion-mass differences exactly the opposite occurs: the isovector *np* phase parameters are *smaller* than the corresponding *pp* phase parameters. This is a unique feature of the potentials presented here.

Defining

$$V(m) = \left(\frac{m}{m_{\pi^\pm}}\right)^2 m\left[\phi_T^0(m,r)S_{12}+\tfrac{1}{3}\phi_C^1(m,r)(\boldsymbol{\sigma}_1\cdot\boldsymbol{\sigma}_2)\right], \quad (14)$$

the OPE potential for *pp* scattering is given by

$$V_{\rm OPE}(pp) = f_\pi^2 V(m_{\pi^0}), \quad (15)$$

whereas for *np* scattering it reads

$$V_{\rm OPE}(np) = -f_\pi^2 V(m_{\pi^0}) \pm 2f_\pi^2 V(m_{\pi^\pm}), \quad (16)$$

where the plus (minus) sign corresponds to total isospin $I = 1\,(0)$. The scaling mass $m_{\pi^\pm}$ in $V(m)$ is introduced in order to make the pseudovector coupling constant f_π dimensionless. It is conventionally chosen to be equal to the charged-pion mass. The explicit distinction between neutral and charged pions implies that the isovector *np* and *pp* OPE potentials are different, and so charge independence is broken. In our present models we assume, however, that the pion-nucleon coupling constants obey charge independence.

B. Nijmegen potential

In this section we briefly discuss the structure of the Nijmegen potential. More details can be found in Refs. [4,18]. The basic functions are the one-boson-exchange (OBE) potential functions with momentum-dependent central terms and exponential form factors. The meson exchanges we include are those due to pseudoscalar mesons (π,η,η'), vector mesons (ρ,ω,ϕ), and scalar mesons (a_0,f_0,ϵ). Here we use the modern nomenclature for the scalar mesons, i.e., $a_0(983)$ corresponds to the δ of Ref. [4], and $f_0(975)$ to the $S^\star$. The ϵ meson would correspond to an $f_0(760)$. No such meson is listed by the Particle Data Group [17]; however, a recent analysis of the $\pi N \to \pi^+\pi^- N$ reaction [19] provides evidence for a scalar-isoscalar resonant state $0^{++}(750)$. In the Nijmegen potentials the ϵ meson corresponds to a broad meson (see below) where the pole in its propagator is chosen to correspond to the pole position in the complex energy plane of the isoscalar $\pi\pi$ S wave [20]. Here we will retain the name of ϵ meson. The aforementioned meson exchanges can be identified with the dominant parts of the lowest-lying meson trajectories in the complex J plane. We furthermore include the dominant $J = 0$ parts of the Pomeron, and of the f_2, f_2', and a_2 tensor-meson trajectories. They give rise to Gaussian potentials.

The meson propagators including the exponential form factor read

$$\Delta(\mathbf{k}^2,m^2,\Lambda^2) = \frac{1}{\mathbf{k}^2+m^2}\, e^{-\mathbf{k}^2/\Lambda^2}. \quad (17)$$

For the Pomeron-type exchanges we have

$$\Delta(\mathbf{k}^2,m_p^2) = \frac{1}{M_p^2}\, e^{-\mathbf{k}^2/4m_p^2}, \quad (18)$$

where m_p has the dimension of a mass and will be called the Pomeron mass, and M_p is a scaling mass, chosen to be the proton mass. The different potential forms are evaluated in momentum space and the resulting expressions are essentially those of Ref. [4] (save some misprints [21]) with the following differences: (i) We explicitly account for the proton and neutron mass difference; (ii) the differences between the neutral and charged pion (see Sec. III A), and between the neutral and charged ρ meson are explicitly included; (iii) we have adjusted the quadratic spin-orbit operator of the potential in momentum space to include the P_5' contribution as in Eq. (4). The effect of the first modification is obviously rather small. The second modification (as well as the first) implies that charge independence is broken in the non-OPE part of the potential as well. For *pp* scattering the potential consists of only neutral-meson exchange, $V_{pp} = V(\text{neutral})$, whereas for *np* scattering it consists of neutral-meson and charged-meson exchange, depending on the total isospin as in Eq. (16),

so $V_{np} = -V(\text{neutral}) \pm 2V(\text{charged})$. This distinction replaces the factor $(\boldsymbol{\tau}_1 \cdot \boldsymbol{\tau}_2)$ used in the old Nijm78 potential. Finally, the third modification means that we have constructed a potential which is exactly equivalent in both momentum space and configuration space, a unique feature of these Nijmegen potentials. For example, for the parametrized Paris potential [7] this is not true since it uses the same parameters in combination with the Q_{12} operator in configuration space as it does with the $(\boldsymbol{\sigma}_1 \cdot \mathbf{n})(\boldsymbol{\sigma}_2 \cdot \mathbf{n})$ operator in momentum space.

Next we briefly discuss the coupling constants. For definitions and references we again refer to Refs. [4,18]. The coupling constants of the pseudoscalar mesons are related via SU(3) and singlet-octet mixing. The octet coupling f_{η_8} is calculated using $\alpha_P = 0.355$ for the $F/(F+D)$ ratio. For the singlet-octet mixing angle we use $\theta_P = -23°$ to define the physical coupling constants f_η and $f_{\eta'}$. This leaves the singlet coupling f_{η_1} and the pion coupling f_π as free input parameters. However, in our partial-wave analysis of the pp scattering data [22], we found for the $pp\pi^0$ coupling constant $f_p^2 = 0.0749(7)$. This value was later confirmed in a combined partial-wave analysis of all pp and np scattering data, assuming charge independence for the pion-nucleon coupling constants [9,11]. There the value $f_\pi^2 = 0.075$ is recommended for the pion-nucleon coupling constant at the pion pole. This is the value we adopt in our construction of the new Nijmegen potentials, and so it is not included as a free parameter.

For the vector mesons we assume that the ρ meson is universally coupled to the isospin current ($\alpha_V^c = 1$) to define the octet coupling g_{V_8}. For the singlet-octet mixing angle we take $\theta_V = 37.5°$, which fixes the physical coupling constants g_ω and g_ϕ in terms of g_ρ and g_{V_1}. The ϕ meson is assumed to have $f_\phi \equiv 0$. The free parameters are now g_ρ, g_{V_1}, f_ρ, and f_ω.

For the scalar mesons we do not apply any constraints for the coupling constants, since the singlet-octet mixing angle for the scalar mesons is still an unsettled problem (see also Ref. [18]). The free parameters are the a_0, f_0, and ϵ coupling constants.

For simplicity we take a single mass parameter m_p for the Pomeron, and for the $J = 0$ parts of the f_2, f_2', and a_2 tensor-meson trajectories. We use two coupling constants: g_{a_2} for the isovector a_2 meson and g_p for the isoscalar and Pomeron exchanges.

For each type of exchange we use an independent cutoff mass, so we have three cutoff parameters Λ_P, Λ_V, and Λ_S. This brings us to a total of 14 free parameters.

We conclude this section with a discussion of the treatment of the broad ρ and ϵ mesons. The width of a broad meson can be accounted for [23–25] by replacing the propagator $\Delta(\mathbf{k}^2) = 1/(\mathbf{k}^2 + m^2)$ of a stable meson by a dispersion integral

$$\Delta(\mathbf{k}^2) = \int_{m_t^2}^{\infty} \frac{\rho(m'^2) dm'^2}{\mathbf{k}^2 + m'^2} , \tag{19}$$

with mass distribution

TABLE I. Values for the parameters of Eq. (22) of the two-pole approximation for the broad ϵ meson and the broad neutral and charged ρ mesons. Masses m and widths Γ are in MeV.

	ϵ	ρ^0	$\rho^\pm$
n	0	1	1
m	760.0	768.7	768.3
Γ	640.0	152.4	149.1
β_1	0.16900	0.26552	0.38755
m_1	487.818	645.377	674.152
β_2	0.61302	0.56075	0.45083
m_2	1021.14	878.367	929.974

$$\rho(m'^2) = \frac{1}{\pi} \frac{\gamma (m'^2 - m_t^2)^{n+1/2}}{(m'^2 - m^2)^2 + \gamma^2 \left(\frac{m'^2}{m^2}\right)^{2n} (m'^2 - m_t^2)^{2n+1}} , \tag{20}$$

and where

$$\gamma = m\Gamma (m^2 - m_t^2)^{-(n+1/2)} . \tag{21}$$

Here Γ denotes the width and $n = 0, 1$ for spin-0 and spin-1 mesons, respectively [23]. The charged ρ meson decays into a neutral and a charged pion and the threshold mass is $m_t = m_{\pi^0} + m_{\pi^\pm}$. The neutral ρ meson cannot decay into two neutral pions and it decays into two charged pions, and so now the threshold mass is $m_t = 2m_{\pi^\pm}$. The ϵ meson is an isoscalar meson which decays into both two neutral or two charged pions in the ratio 1:2. In our present models these distinctions have been explicitly accounted for, which is another extension of the old Nijm78 model.

The configuration-space potential due to the exchange of a broad meson is calculated exactly. This exact potential is then approximated by the sum of two potentials of stable mesons [24]

$$\int_{m_t}^{\infty} dm' 2m' \rho(m'^2) m' \phi_C^0(m', r) \approx \beta_1 m_1 \phi_C^0(m_1, r) + \beta_2 m_2 \phi_C^0(m_2, r) . \tag{22}$$

Fitting from 0–2 fm yields the values as given in Table I.

C. Regularized Reid potential

A disadvantage of the original Reid68 potential is that, at the time of its construction, the quality of the np data was very poor. As a consequence, the Reid68 potential can no longer properly describe the numerous new and much more accurate np data. Another disadvantage is that the Reid68 potential has an r^{-1} singularity in all partial waves. Here we present an updated version of the Reid potential, where these singularities have been removed via the inclusion of a dipole form factor. With this choice, the tensor potential now also vanishes at the origin, as it should.

As is the case for the original Reid68 potential, the

OPE potential is explicitly included, while we now account for the neutral-pion and charged-pion mass differences as in Eqs. (14)–(16). For the pion-nucleon coupling constant at the pion pole we take [9,11] $f_\pi^2 = 0.075$, and for the dipole cutoff parameter we choose $\Lambda = 8m_\pi$. In the OPE potential (14) we use ϕ_C^1 only for the S waves. For all other partial waves, we found it more convenient to use ϕ_C^0 instead of ϕ_C^1. Note that ϕ_C^1 equals ϕ_C^0 up to a modified δ function [see Eq. (11)], and that this modified δ function is screened by the centrifugal barrier for all these other partial waves, except the S waves.

Starting with this OPE potential, the potential in each partial wave can now be extended by choosing a convenient combination of central, tensor, and spin-orbit functions with arbitrary masses and cutoff parameters. In the construction presented in the following we (more or less arbitrarily) settled for integer multiples of a mean pion mass $\overline{m} = (m_{\pi^0} + 2m_{\pi^\pm})/3$, while the cutoff mass in the dipole form factor is chosen to be $\Lambda = 8\overline{m}$ everywhere. For notational reasons we next define

$$\begin{aligned} Y(p) &= p\overline{m}\,\phi_C^0(p\overline{m}, r), \\ Z(p) &= p\overline{m}\,\phi_T^0(p\overline{m}, r), \\ W(p) &= p\overline{m}\,\phi_{\rm SO}^0(p\overline{m}, r), \end{aligned}$$

with p an integer and ϕ_X^0 given by Eqs. (9) and (12). For the coefficients multiplying these functions, we use A_{ip} for the isovector potentials, whereas the coefficients B_{ip} are for the isoscalar and $np\ ^1S_0$ potentials. The index i subsequently labels the different partial waves. For the total potential in a particular partial wave one should, of course, add the appropriate OPE potential as given by Eqs. (14)–(16).

For the non-OPE parts in the isovector singlet partial waves ($I = 1$, $S = 0$, $L = J$) we use

$$\begin{aligned} V_{pp}(^1S_0) &= A_{12}Y(2) + A_{13}Y(3) + A_{14}Y(4) \\ &\quad + A_{15}Y(5) + A_{16}Y(6)\ , \\ V_{np}(^1S_0) &= B_{13}Y(3) + B_{14}Y(4) + B_{15}Y(5) + B_{16}Y(6)\ , \\ V(^1D_2) &= A_{24}Y(4) + A_{25}Y(5) + A_{26}Y(6)\ , \\ V(^1G_4) &= A_{33}Y(3)\ , \\ V(^1J_J) &= V_{pp}(^1S_0) \quad \text{for } J \geq 6\ , \end{aligned} \tag{23}$$

where the distinction between the pp and $np\ ^1S_0$ potentials is necessary because of the well-known breaking of charge independence in the pp and $np\ ^1S_0$ partial waves. The coefficients A_{ip} and B_{ip} are to be fitted. The presence of the two-pion range piece $A_{12}Y(2)$ in the $pp\ ^1S_0$ potential is purely coincidental, and was only included to improve the quality of the fit. A similar term in the $np\ ^1S_0$ was much less effective, and so we decided to leave it out.

For the non-OPE parts in the isoscalar singlet partial waves ($I = 0$, $S = 0$, $L = J$) we use

$$\begin{aligned} V(^1P_1) &= B_{23}Y(3) + B_{24}Y(4) + B_{25}Y(5) + B_{26}Y(6)\ , \\ V(^1F_3) &= B_{33}Y(3) + B_{35}Y(5)\ , \\ V(^1J_J) &= V(^1P_1) \quad \text{for } J \geq 5\ . \end{aligned} \tag{24}$$

For the isovector triplet uncoupled partial waves ($I = 1$, $S = 1$, $L = J$) we use

$$\begin{aligned} V(^3P_0) &= A_{43}Y(3) + A_{45}Y(5) + A_{4z3}Z(3)\ , \\ V(^3P_1) &= A_{53}Y(3) + A_{55}Y(5) + A_{5z3}Z(3)\ , \\ V(^3F_3) &= A_{63}Y(3)\ , \end{aligned} \tag{25}$$

and the isoscalar triplet uncoupled partial waves ($I = 0$, $S = 1$, $L = J$) are parametrized as

$$\begin{aligned} V(^3D_2) &= B_{43}Y(3) + B_{45}Y(5) + B_{4z3}Z(3)\ , \\ V(^3G_4) &= B_{53}Y(3)\ . \end{aligned} \tag{26}$$

Following the parametrization of the original Reid68 potential, the non-OPE potential in the triplet coupled partial waves ($S = 1$, $L = J \pm 1$) is parametrized as

$$V = V_C + V_T S_{12} + V_{\rm SO}\mathbf{L}\cdot\mathbf{S}\ , \tag{27}$$

where the isovector ($I = 1$) potentials are given by

$$\begin{aligned} V_C &= A_{73}Y(3) + A_{74}Y(4) + A_{75}Y(5) + A_{76}Y(6)\ , \\ V_T &= A_{7z4}Z(4) + A_{7z6}Z(6)\ , \\ V_{\rm SO} &= A_{7w3}W(3) + A_{7w5}W(5) \quad \text{for } J = 2\ , \\ V_{\rm SO} &= A_{8w3}W(3) \quad \text{for } J = 4\ , \end{aligned} \tag{28}$$

and the isoscalar ($I = 0$) potentials read

$$\begin{aligned} V_C &= B_{62}Y(2) + B_{63}Y(3) + B_{64}Y(4) \\ &\quad + B_{65}Y(5) + B_{66}Y(6)\ , \\ V_T &= B_{6z4}Z(4) + B_{6z6}Z(6)\ , \\ V_{\rm SO} &= B_{6w3}W(3) + B_{6w5}W(5) \quad \text{for } J = 1\ , \\ V_{\rm SO} &= B_{7w3}W(3) + B_{7w5}W(5) \quad \text{for } J = 3\ . \end{aligned} \tag{29}$$

Finally, for the triplet isovector partial waves ($I = 1$, $S = 1$) with $J \geq 5$ we use Eq. (27) with the central and tensor potentials of Eq. (28), and the spin-orbit potential equal to zero. Similarly, for the triplet isoscalar partial waves ($I = 0$, $S = 1$) with $J \geq 5$ we use the central and tensor potentials of Eq. (29). This choice is analogous to the extension of the Reid68 potential to the higher partial waves as given by Day [26].

IV. RESULTS

The parameters of the potential models are optimized by minimizing the χ^2 in a direct fit to the data. Since the scattering data are spread over a large number of energies (about 200 different energies for the pp data and almost 400 different energies for the np data in the 0–350 MeV energy range) and the phase parameters need to be calculated up to at least $J \approx 6$, the Schrödinger equation then has to be solved a very large number of times. This approach, therefore, is not very practical when the model parameters do not yet have reasonable values and, consequently, the χ^2 is still very high. A more convenient approach is to start with the Nijmegen representation [1] of the χ^2 hypersurface of the scattering data. It is obtained from the 10 single-energy analyses and consists of

10 sets of phase parameters and the error matrix, each at a different energy. The error matrix is the inverse of half the second-derivative matrix of the χ^2 hypersurface with respect to the phase parameters up to $J = 4$ within the energy bin of the single-energy analysis. This χ^2 hypersurface is, in principle, independent of the particular partial-wave analysis. In practice the representation we use is somewhat dependent on the Nijmegen multienergy analysis. The crucial point is, however, that it provides a very good and concise representation of the scattering data. For each change in the model parameters we need to solve the Schrödinger equation for all partial waves up to $J = 4$ at only 10 different energies, which allows for a much quicker optimization for the parameters of the potential model.

In the last stage of the fitting procedure the potential parameters have been further optimized in a very time-consuming direct fit to the data. In this case we use the potential model in all partial waves with $J \leq 6$, whereas in the higher partial waves we include OPE only. The final $\chi^2_{\min}$ of the potential should be obtained from this direct comparison with the experimental data.

A. Nijm92*pp*

Our first improvement of the Nijm78 potential [4] was already started several years ago, when we constructed an update to the *pp* data of the Nijm78 potential. This potential has been used in the Nijmegen analyses [9–11] to parametrize the *np* isovector lower partial waves (except the *np* $^1S_0$). In our latest analysis [1] (PWA93) we refer to it as the Nijm92*pp* potential. We found that a good fit to the *pp* data could be obtained using one cutoff parameter $\Lambda = 827.53$ MeV for all three types of meson exchanges. Some of the coupling constants were not refitted, but were kept at the values of the original Nijm78 potential. The reason is that, when we only fit to the *pp* data, we cannot incorporate the isospin dependence of the isovector exchanges (there are only $I = 1$ partial waves). A direct comparison of this Nijm92*pp* potential with the *pp* data yields $\chi^2 = 2487.1$ for 1787 data, which means $\chi^2/N_{pp} = 1.4$.

B. Nijm93

Now that the Nijmegen analysis of the *np* data is also finished [1] and we have carefully scrutinized the *np* database, we can extend the update of the Nijm78 potential to include the fit to the *np* scattering data as well. This model we refer to as Nijm93.

As already mentioned in Sec. III C, the *np* $^1S_0$ partial wave has to be parametrized separately. The reason is that there is clear evidence for breaking of charge independence in the $^1S_0$ scattering lengths a_{pp} and a_{np}. This difference in scattering lengths carries over into an approximately 2° phase-shift difference between the *pp* and *np* $^1S_0$ phase shifts at higher energies. This difference cannot be explained as being only due to the difference between the *pp* and *np* OPE potentials. Allowing for a different value for the neutral-pion and charged-pion coupling constants does not help either, because the scattering lengths are very insensitive to these kind of changes. To accommodate the *pp* and *np* $^1S_0$ differences, we therefore introduce a purely phenomenological breaking of charge independence between the ρ^0 and $\rho^\pm$ coupling constants. This breaking of charge independence is *only* assumed in the $^1S_0$ partial wave; for all other partial waves the ρ^0 and $\rho^\pm$ coupling constants are taken to be the same.

The parameters for the Nijm93 potential, rounded to four or five significant figures, can be found in Table II, where the meson masses are the masses as listed by the 1990 Particle Data Group [17]. The coupling constants are the values at $\mathbf{k}^2 = 0$. The pion coupling constants are fixed at $f^2 = 0.075$ at the corresponding pion pole $\mathbf{k}^2 = -m^2_{\pi^0}$ or $\mathbf{k}^2 = -m^2_{\pi^\pm}$; hence the different entries for neutral- and charged-pion exchange at $\mathbf{k}^2 = 0$. The ϵ and Pomeron coupling constants are rather large, whereas the ω coupling constant is reasonably small. For the ρ coupling constants we find $(f/g)_\rho = 4.094$, which is close to the value 3.7 from naive vector-meson dominance of the isovector electromagnetic form factors of the nucleon.

For the Nijm93 potential we find $\chi^2(pp) = 3175.6$ for 1787 *pp* data and $\chi^2(np) = 4848.4$ for 2514 *np* data. So for the *pp* data $\chi^2/N_{pp} = 1.8$, for the *np* data $\chi^2/N_{np} = 1.9$, and for all *NN* data $\chi^2/N_{\text{data}} = 1.87$. We find that this 15-parameter conventional meson-exchange potential cannot do better than $\chi^2/N_{\text{data}} \approx 1.87$, a result which is also found for similar potential models such as the Paris80 and all the Bonn potentials. Apparently, the conventional meson-exchange potentials cannot compete in quality with the Nijmegen PWA93. This indicates that these models lack some important physics.

TABLE II. Masses and meson-nucleon coupling constants at $\mathbf{k}^2 = 0$ for the Nijm93 potential. For the *np* $^1S_0$ partial wave the coupling constants of the charged-rho meson are increased by 4.371% (see text). P in the last line denotes the Pomeron. Note that $(f/g)_\rho = 4.094$.

	m (MeV)	g^2	f^2
$\pi^\pm$	139.5675		0.07395
π^0	134.9739		0.07402
η	548.8		0.01514
η'	957.5		0.01466
Λ_P	1177.11		
$\rho^\pm$	768.3, $\Gamma = 149.1$	0.8481	14.217
ρ^0	768.7, $\Gamma = 152.4$	0.8481	14.217
ω	781.95	9.1765	0.3383
ϕ	1019.412	0.0985	0
Λ_V	904.50		
$a_0^\pm, a_0^0$	983.3	1.9174	
ϵ	760.0, $\Gamma = 640.0$	28.196	
f_0	975.6	12.142	
Λ_S	554.40		
a_2	208.16	0.0486	
P, f_2, f_2'	208.16	27.339	

C. Nijm I and Nijm II

In order to be able to construct a potential model which is of almost the same quality as the Nijmegen PWA93 ($\chi^2/N_{\rm data} \approx 1$), we follow a different approach and take advantage of the success of the Reid68 potential. We expect that, when we start with the Nijmegen potential (which already has a reasonable χ^2 on the *pp* data), we can construct a Reid-like potential where in each partial wave we probably need to adjust only a few parameters in order to arrive at $\chi^2/N_{\rm data} \approx 1$. The potential forms are then given by a set of slightly adjusted Nijmegen potentials, each representing one particular partial wave. Starting with the parameters of the Nijm92*pp* potential [12], we find that for most partial waves an adjustment of the f_ρ and g_ϵ coupling constants already gives very good results. Counting all parameters which have been adjusted in the fit of each partial wave, we arrive at a total of 41 parameters. This should be compared with the 39 parameters used in the Nijmegen PWA93.

In the last stage, the parameters of this Reid-like potential are optimized in a direct fit to the data. The potential is then used in all partial waves up to $J = 6$ simultaneously. This model we refer to as Nijm I. It has $\chi^2(pp) = 1795.8$ and $\chi^2(np) = 2627.3$, and so $\chi^2/N_{\rm data} = 1.03$ on all *pp* and *np* scattering data.

We have also constructed a local Reid-like Nijmegen potential, where we leave out the explicit momentum-dependent terms which give rise to nonlocal contributions to the configuration-space potential as expressed in Eq. (13). We follow the same procedure as for the nonlocal Nijm I potential. First, the parameters are adjusted in a fit to the representation of the χ^2 hypersurface, and then further optimized in a direct fit to the data. For this local potential, denoted by Nijm II, we use a total of 47 parameters and we find $\chi^2(pp) = 1795.8$ and $\chi^2(np) = 2625.7$, and so $\chi^2/N_{\rm data} = 1.03$.

Although these potentials are purely phenomenological (except for the correct OPE tail) and the coupling constants have no physical meaning, these potentials are the first to give an excellent description of the *NN* scattering data. They have already been used successfully in three- and many-body calculations [27,28].

D. Reid93

Finally, we have constructed an updated Reid potential based on the original Reid68 potential. This regularized version, denoted by Reid93 and discussed in Sec. III C, gives an equally good description of the data as do the Nijm I and Nijm II potentials. The 50 phenomenological potential parameters A_{ip} and B_{ip} were fitted to the data, resulting in $\chi^2(pp) = 1795.1$ and $\chi^2(np) = 2624.6$, and so also for this potential $\chi^2/N_{\rm data} = 1.03$. This Reid93 potential has been used in a triton calculation as well [27].

E. Comparison of the potentials

The results of the nonlocal Nijm I potential, the local Nijm II potential, and the local Reid93 potential are summarized in Table III. The results of the Nijmegen PWA93 are shown for comparison. Although $\chi^2/N_{\rm data}$ for these three potentials is already very good, their description of the *np* data is still not as good as the description of these *np* data in the partial-wave analysis. Here we should also mention that we did not do a thorough investigation into the minimum number of parameters required to get these results (as we did for the partial-wave analysis). The reason is that in order to do this properly, all potential parameters have to be fitted simultaneously to all *NN* data. But we found it more successful to do a large number of fits where in each separate run only a (completely arbitrary) subset of the potential parameters was optimized. Therefore, we cannot rule out the possibility that an equally good fit can be obtained with a few parameters less.

TABLE III. χ^2 for the new potential models in comparison with the Nijmegen multienergy analysis [1] PWA93. We also show the number of parameters ($N_{\rm par}$) for each model.

	PWA93	Nijm I	Nijm II	Reid93	Nijm93
pp	1787.0	1795.8	1795.8	1795.1	3175.6
np	2489.2	2627.3	2625.7	2624.6	4848.4
Total	4276.2	4423.1	4421.5	4419.7	8023.9
$N_{\rm par}$	39	41	47	50	15
$\chi^2/N_{\rm data}$	0.99	1.03	1.03	1.03	1.87

As already mentioned in the Introduction, these new potentials (except Nijm93) are in a sense alternative partial-wave analyses. The differences between the phase parameters of the potentials and the phase parameters of the Nijmegen PWA93 are shown in Tables IV and V. These differences provide an indication for the systematic error on the results of the Nijmegen PWA93. For the *np* phase parameters the differences at some energies (especially with the Reid93 potential) are relatively large. However, one has to bear in mind that $\chi^2(np)$ of the potential models is still substantially higher than that of the multienergy partial-wave analysis. On the

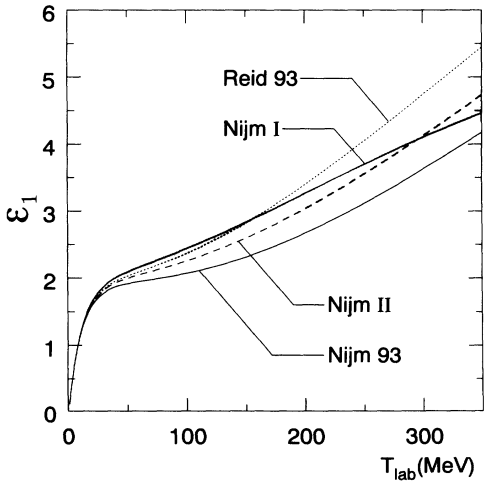

FIG. 1. The mixing parameter ϵ_1 of the various potentials and of the Nijmegen PWA93. The shaded band denotes the statistical error on ϵ_1 as obtained in the Nijmegen partial-wave analysis.

other hand, the variation in the mixing parameter ϵ_1 is small. It has often been claimed that this mixing parameter is ill determined and a wide range of values from potential models seemed acceptable (see, e.g., Refs. [6,8]). However, in our publication of the Nijmegen PWA93 we already argued that ϵ_1 is in fact known very accurately. This is confirmed in Fig. 1, where we note that the results of the Nijm I and Nijm II models lie essentially within the *statistical* uncertainty as obtained in the Nijmegen PWA93. Above 150 MeV, the result of the Reid93 model rises too strongly but is still within 2.5 standard deviations of the Nijmegen PWA93.

The potentials between 0 and 2 fm for the singlet, triplet uncoupled, and triplet coupled *np* partial waves are shown in Figs. 2, 3, and 4, respectively. For the nonlocal potential Nijm I we plot $V/(1 + 2\varphi)$, which more or less represents the effective potential when nonlocal terms are present (see Refs. [16,4]). For coupled channels, the potential is a 2×2 matrix and the ε_1 and ε_2 plots in Fig. 4 represent the off-diagonal elements of the potential. The main differences between the potentials show up in the inner region, i.e., for $r < 1$ fm. In general, the nonlocal Nijm I potential is much softer than the local Nijm II and Reid93 potentials, while the Nijm II

TABLE IV. *pp* phase shifts in degrees. For each energy the rows give the values from the Nijmegen multienergy partial-wave analysis [1], the nonlocal Nijm I potential, the local Nijm II potential, and the Reid93 potential, respectively.

$T_{\rm lab}$	$^1S_0$	$^1D_2$	$^3P_0$	$^3P_1$	$^3P_2$	ε_2	$^3F_2$
1	32.77	0.00	0.13	−0.08	0.01	−0.00	0.00
	32.79	0.00	0.13	−0.08	0.01	−0.00	0.00
	32.80	0.00	0.13	−0.08	0.01	−0.00	0.00
	32.79	0.00	0.13	−0.08	0.01	−0.00	0.00
5	54.85	0.04	1.58	−0.90	0.21	−0.05	0.00
	54.88	0.04	1.58	−0.90	0.22	−0.05	0.00
	54.91	0.04	1.57	−0.89	0.22	−0.05	0.00
	54.85	0.04	1.57	−0.90	0.21	−0.05	0.00
10	55.22	0.17	3.73	−2.06	0.65	−0.20	0.01
	55.25	0.17	3.73	−2.05	0.66	−0.20	0.01
	55.28	0.17	3.70	−2.04	0.65	−0.20	0.01
	55.22	0.16	3.71	−2.05	0.65	−0.20	0.01
25	48.66	0.70	8.58	−4.93	2.49	−0.81	0.10
	48.68	0.70	8.60	−4.91	2.50	−0.81	0.11
	48.72	0.70	8.52	−4.89	2.49	−0.81	0.11
	48.71	0.69	8.60	−4.90	2.49	−0.80	0.10
50	38.92	1.71	11.47	−8.32	5.85	−1.71	0.34
	38.91	1.71	11.55	−8.31	5.85	−1.70	0.34
	38.92	1.70	11.48	−8.30	5.84	−1.70	0.34
	39.03	1.68	11.67	−8.30	5.83	−1.69	0.34
100	24.98	3.79	9.45	−13.26	11.01	−2.66	0.82
	24.96	3.73	9.50	−13.30	10.96	−2.63	0.82
	24.91	3.75	9.55	−13.33	10.97	−2.64	0.83
	25.09	3.71	9.79	−13.30	10.97	−2.61	0.81
150	14.77	5.61	4.74	−17.43	13.98	−2.87	1.20
	14.79	5.60	4.63	−17.51	13.94	−2.87	1.19
	14.70	5.61	4.77	−17.54	13.95	−2.87	1.20
	14.83	5.55	4.97	−17.49	13.96	−2.85	1.16
200	6.57	7.06	−0.37	−21.25	15.63	−2.76	1.42
	6.66	7.20	−0.63	−21.32	15.65	−2.80	1.39
	6.56	7.15	−0.47	−21.29	15.63	−2.79	1.42
	6.62	7.08	−0.32	−21.26	15.63	−2.77	1.36
250	−0.30	8.27	−5.43	−24.77	16.59	−2.54	1.47
	−0.20	8.50	−5.72	−24.81	16.65	−2.62	1.39
	−0.25	8.41	−5.61	−24.67	16.61	−2.61	1.44
	−0.23	8.35	−5.45	−24.71	16.59	−2.55	1.39
300	−6.14	9.42	−10.39	−27.99	17.17	−2.34	1.34
	−6.18	9.52	−10.49	−28.02	17.26	−2.41	1.20
	−6.12	9.42	−10.49	−27.71	17.21	−2.41	1.29
	−6.10	9.40	−10.29	−27.86	17.15	−2.26	1.25
350	−11.11	10.69	−15.30	−30.89	17.54	−2.21	1.04
	−11.51	10.28	−14.94	−30.98	17.63	−2.23	0.86
	−11.28	10.24	−15.08	−30.45	17.61	−2.23	0.98
	−11.22	10.30	−14.80	−30.77	17.49	−1.95	0.95

TABLE V. *np* phase shifts in degrees. For each energy the rows give the values from the Nijmegen multienergy partial-wave analysis [1], the nonlocal Nijm I potential, the local Nijm II potential, and the Reid93 potential, respectively.

T_{lab}	$^1S_0$	$^3P_0$	$^1P_1$	$^3P_1$	$^3S_1$	ε_1	$^3D_1$	$^1D_2$	$^3D_2$	$^3P_2$	ε_2	$^3F_2$
1	62.07	0.18	−0.19	−0.11	147.75	0.11	−0.01	0.00	0.01	0.02	−0.00	0.00
	62.11	0.18	−0.19	−0.11	147.76	0.10	−0.01	0.00	0.01	0.02	−0.00	0.00
	62.09	0.18	−0.19	−0.11	147.75	0.10	−0.01	0.00	0.01	0.02	−0.00	0.00
	61.89	0.18	−0.19	−0.11	147.73	0.10	−0.01	0.00	0.01	0.02	−0.00	0.00
5	63.63	1.63	−1.49	−0.94	118.18	0.67	−0.18	0.04	0.22	0.25	−0.05	0.00
	63.74	1.62	−1.50	−0.93	118.19	0.67	−0.18	0.04	0.22	0.25	−0.05	0.00
	63.66	1.60	−1.52	−0.93	118.17	0.66	−0.18	0.04	0.22	0.25	−0.05	0.00
	63.23	1.61	−1.48	−0.93	118.15	0.66	−0.18	0.04	0.22	0.26	−0.05	0.00
10	59.95	3.65	−3.04	−2.06	102.61	1.16	−0.68	0.16	0.85	0.71	−0.18	0.01
	60.10	3.64	−3.08	−2.05	102.62	1.15	−0.68	0.16	0.85	0.71	−0.18	0.01
	59.99	3.61	−3.11	−2.04	102.59	1.13	−0.67	0.16	0.85	0.71	−0.18	0.01
	59.46	3.64	−3.04	−2.05	102.59	1.14	−0.67	0.16	0.85	0.72	−0.18	0.01
25	50.90	8.13	−6.31	−4.88	80.63	1.79	−2.80	0.68	3.71	2.56	−0.76	0.09
	51.04	8.16	−6.42	−4.86	80.59	1.77	−2.80	0.69	3.72	2.57	−0.75	0.09
	50.88	8.09	−6.51	−4.84	80.56	1.73	−2.80	0.68	3.72	2.56	−0.75	0.09
	50.41	8.24	−6.37	−4.85	80.63	1.74	−2.75	0.67	3.73	2.61	−0.75	0.09
50	40.54	10.70	−9.67	−8.25	62.77	2.11	−6.43	1.73	8.97	5.89	−1.63	0.30
	40.56	10.81	−9.80	−8.25	62.64	2.09	−6.45	1.72	8.98	5.88	−1.61	0.31
	40.35	10.76	−9.96	−8.24	62.62	2.00	−6.45	1.72	8.97	5.87	−1.62	0.31
	40.18	11.13	−9.89	−8.26	62.78	2.03	−6.31	1.69	9.00	6.00	−1.60	0.30
100	26.78	8.46	−14.52	−13.24	43.23	2.42	−12.24	3.90	17.27	10.94	−2.58	0.76
	26.44	8.57	−14.42	−13.30	42.98	2.44	−12.26	3.83	17.26	10.89	−2.54	0.76
	26.18	8.65	−14.59	−13.33	42.95	2.25	−12.31	3.85	17.22	10.88	−2.54	0.77
	26.32	9.22	−14.91	−13.38	43.18	2.36	−12.07	3.79	17.12	11.21	−2.54	0.74
150	16.93	3.69	−18.65	−17.46	30.72	2.75	−16.49	5.79	22.12	13.84	−2.80	1.12
	16.33	3.67	−18.23	−17.56	30.47	2.83	−16.45	5.77	22.15	13.80	−2.79	1.11
	16.02	3.83	−18.32	−17.59	30.40	2.59	−16.61	5.78	22.05	13.78	−2.78	1.12
	16.11	4.47	−18.91	−17.68	30.67	2.82	−16.30	5.68	21.72	14.27	−2.82	1.08
200	8.94	−1.44	−22.18	−21.30	21.22	3.13	−19.71	7.29	24.50	15.46	−2.70	1.33
	8.27	−1.60	−21.51	−21.41	21.08	3.27	−19.62	7.43	24.61	15.48	−2.73	1.28
	7.92	−1.42	−21.52	−21.38	20.98	3.03	−19.85	7.38	24.49	15.42	−2.71	1.31
	7.83	−0.74	−22.15	−21.55	21.31	3.40	−19.46	7.26	23.96	16.01	−2.79	1.27
250	1.96	−6.51	−25.14	−24.84	13.39	3.56	−22.21	8.53	25.40	16.39	−2.49	1.35
	1.48	−6.69	−24.28	−24.93	13.46	3.70	−22.13	8.78	25.48	16.47	−2.56	1.26
	1.10	−6.55	−24.22	−24.78	13.35	3.55	−22.34	8.68	25.46	16.39	−2.54	1.32
	0.86	−5.80	−24.71	−25.08	13.81	4.05	−21.84	8.55	24.81	17.02	−2.61	1.28
300	−4.46	−11.47	−27.58	−28.07	6.60	4.03	−24.14	9.69	25.45	16.95	−2.30	1.19
	−4.43	−11.46	−26.52	−28.17	7.00	4.10	−24.21	9.82	25.32	17.08	−2.36	1.06
	−4.84	−11.43	−26.43	−27.85	6.90	4.12	−24.26	9.73	25.52	16.99	−2.35	1.14
	−5.17	−10.57	−26.69	−28.31	7.55	4.74	−23.64	9.63	24.84	17.64	−2.36	1.12
350	−10.58	−16.39	−29.66	−30.97	0.50	4.57	−25.57	10.96	25.08	17.31	−2.18	0.87
	−9.70	−15.90	−28.25	−31.14	1.36	4.47	−26.00	10.60	24.48	17.44	−2.19	0.69
	−10.10	−16.01	−28.17	−30.60	1.30	4.74	−25.74	10.59	25.02	17.40	−2.18	0.81
	−10.47	−15.02	−28.15	−31.27	2.20	5.45	−25.00	10.55	24.40	18.03	−2.09	0.82

potential is again much softer than the Reid93 potential. The reason for this softness of the Nijmegen potentials is the exponential form factor.

Finally, all potential models have been fitted to the deuteron binding energy $B = 2.224\,575(9)$ MeV [29] using relativistic kinematics, i.e.,

$$B = M_p + M_n - \sqrt{M_p^2 - \kappa^2} - \sqrt{M_n^2 - \kappa^2}\ ,$$

rather than $B = \kappa^2/2M_r$. We also constructed versions of the Nijm I and Nijm II potentials to accommodate the latter nonrelativistic form. In any case the value $B = 2.224\,575$ MeV is exactly reproduced to this accuracy. Some of the other deuteron parameters are listed in Table VI. The different potential models all give very similar results. Because we consider the potentials Nijm I, Nijm II, and Reid93 as alternative partial-wave analyses, the values of the deuteron parameter η, A_S, and N^2 given by these potentials are new experimental determinations of these quantities. For the D/S-state ratio η we find $\eta = 0.0252(1)$ in good agreement with the recent determination by Rodning and Knutson [30] of $\eta = 0.0256(4)$. For the asymptotic S-state normalization A_S we obtain $A_S = 0.8843(10)$ fm$^{-1/2}$, which is in agreement with the determination by Kermode *et al.* [31] of $A_S = 0.8883(44)$ fm$^{-1/2}$. This results in $N^2 = A_S^2(1+\eta^2) = 0.7825(20)$ fm^{-1}. However, there have been other experimental determinations of these quantities which are not always in agreement with the values quoted above. For a more complete list of these experimental determinations and a discussion of the differences between them, we refer to Ref. [32], and references cited therein. A direct comparison of our value $Q_d = 0.271(1)$ fm^2 of the deuteron quadrupole mo-

TABLE VI. Deuteron properties of the potential models: D/S-ratio η, asymptotic S-state normalization A_S in fm$^{-1/2}$, wave-function normalization N^2 in fm^{-1}, D-state probability P_d in %, and quadrupole moment Q_d in fm^2.

	Nijm I	Nijm II	Reid93	Nijm93
η	0.0253	0.0252	0.0251	0.0252
A_S	0.8841	0.8845	0.8853	0.8842
N^2	0.7821	0.7828	0.7843	0.7823
P_d	5.664	5.635	5.699	5.755
Q_d	0.2719	0.2707	0.2703	0.2706

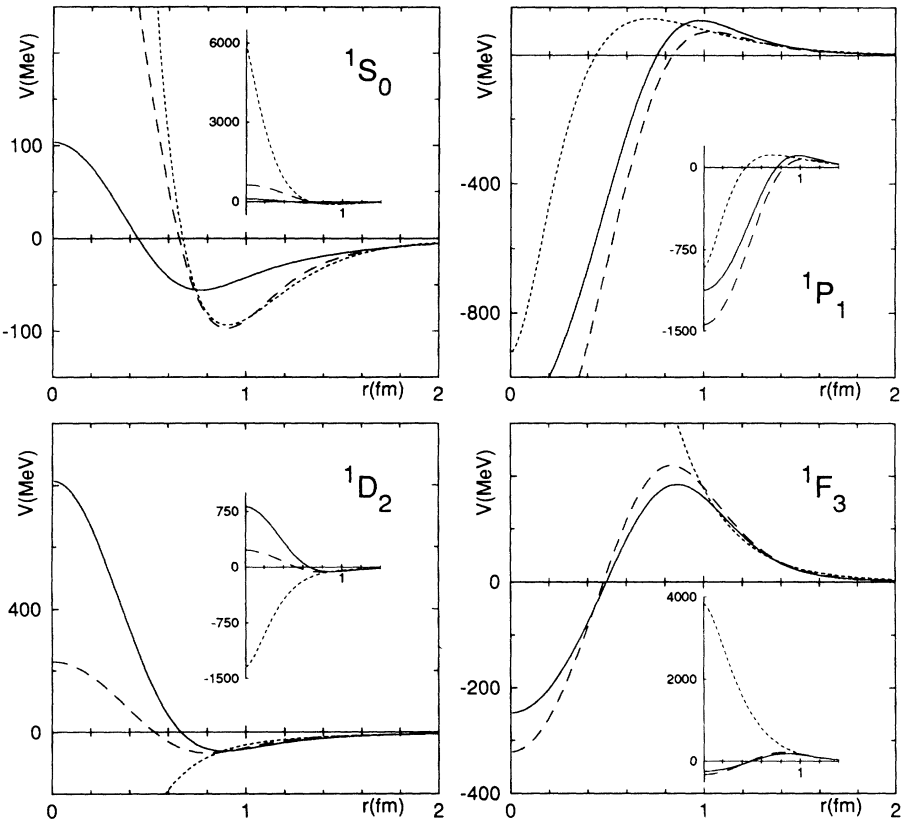

FIG. 2. The new Nijmegen potentials in the np singlet partial waves up to $J = 3$. Solid lines, Nijm I; dashed line, Nijm II; dotted line, Reid93.

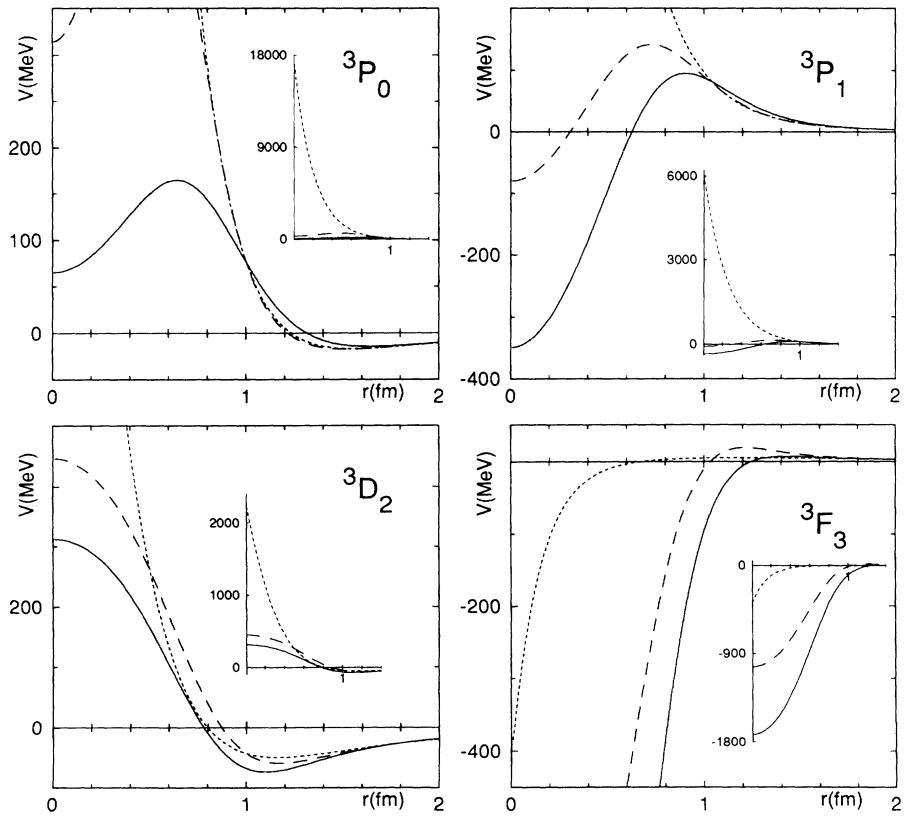

FIG. 3. The new Nijmegen potentials in the np triplet uncoupled partial waves up to $J = 3$. Solid line, Nijm I; dashed line, Nijm II; dotted line, Reid93.

ment with the experimental value 0.2859(3) fm^2 of [33] is only possible after all possible corrections have been accounted for, which is outside the scope of this paper. However, we would like to turn the argument around and suggest that these corrections must obviously be about 0.015 fm^2. It is quite interesting to see that for our best potentials the D-state probability is $P_d = 5.665(30)\%$. The deuteron parameters as well as the results for the scattering lengths for both the potential models and the Nijmegen PWA93 will be discussed in more detail elsewhere [34]. These potentials were used [27] in calculations of the triton binding energy. It turned out that all these potentials underbind the triton by roughly 800 keV, a result which can be expected from their P_d values.

V. CONCLUSIONS

In this paper we presented an update Nijm93 of the old Nijm78 *NN* potential. It contains the correct OPE tail and has $\chi^2/N_{\rm data} = 1.87$. Although it cannot compete in quality with the Nijmegen partial-wave analysis (a feature apparently all conventional meson-exchange potentials suffer from), the description of the *np* data of the new Nijm93 model is substantially better than that of the original Nijm78 potential, which was fitted to the old 1969 Livermore database [35]. Here we would also like to point out that in the Nijm93 model we do not include two-meson-exchange contributions such as $\pi\pi$ and $\pi\rho$ exchange, and we still get a reasonable description of the $^1P_1$ and $^3D_2$ phase shifts. This is in contrast to

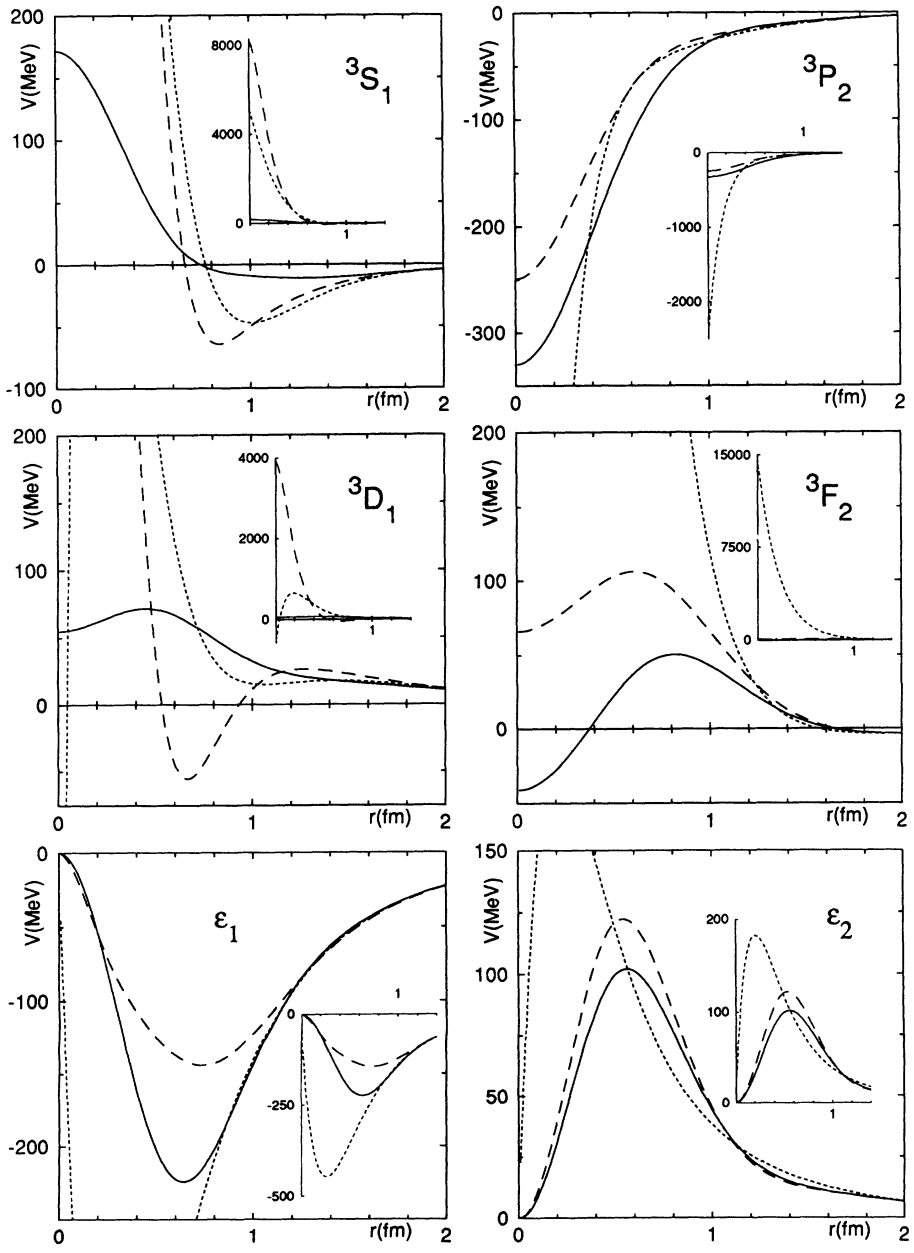

FIG. 4. The new Nijmegen potentials in the *np* triplet coupled partial waves with $J = 1$ and $J = 2$. Solid line, Nijm I; dashed line, Nijm II; dotted line, Reid93.

claims made in the literature [6,8] that this is impossible. However, this result is obtained at the cost of having a rather large value for the pseudoscalar (pion) cutoff mass of $\Lambda_P = 1177.11$ MeV.

We have also presented three new high-quality *NN* potentials. The Nijm I potential is a nonlocal Reid-like potential where each of the lower partial waves up to $J = 4$ is parametrized separately. For the higher partial waves we use the parameters of the Nijm92*pp* potential, which is an update to the *pp* data of the original Nijm78 potential. The Nijm II potential is a local Reid-like potential, and does not contain any explicit momentum-dependent terms. Both potentials fit the *NN* scattering data with a nearly optimal $\chi^2_{\rm min}/N_{\rm data} = 1.03$. A regularized update of the Reid potential, denoted by Reid93, gives the same excellent $\chi^2_{\rm min}/N_{\rm data} = 1.03$.

Computer codes for these Nijmegen potentials Nijm I, Nijm II, and Nijm93, and for the regularized Reid93 potential, in configuration space as well as in momentum space, can be readily obtained via anonymous FTP from thef-nym.sci.kun.nl.

ACKNOWLEDGMENTS

We would like to thank Dr. J. L. Friar and Dr. Th. A. Rijken for many helpful discussions. Part of this work was included in the research program of the Stichting voor Fundamenteel Onderzoek der Materie (FOM) with financial support from the Nederlandse Organisatie voor Wetenschappelijk Onderzoek (NWO). One of us (V.G.J.S.) would also like to thank the Australian Research Council for financial support.

[1] V.G.J. Stoks, R.A.M. Klomp, M.C.M. Rentmeester, and J.J. de Swart, Phys. Rev. C **48**, 792 (1993).
[2] V. Stoks and J.J. de Swart, Phys. Rev. C **47**, 761 (1993).
[3] R.V. Reid, Jr., Ann. Phys. (N.Y.) **50**, 411 (1968).
[4] M.M. Nagels, T.A. Rijken, and J.J. de Swart, Phys. Rev. D **17**, 768 (1978).
[5] J. Haidenbauer and K. Holinde, Phys. Rev. C **40**, 2465 (1989).
[6] R. Machleidt, K. Holinde, and Ch. Elster, Phys. Rep. **149**, 1 (1987).
[7] M. Lacombe, B. Loiseau, J.M. Richard, R. Vinh Mau, J. Côté, P. Pirès, and R. de Tourreil, Phys. Rev. C **21**, 861 (1980).
[8] R. Machleidt, Adv. Nucl. Phys. **19**, 189 (1989).
[9] R.A.M. Klomp, V.G.J. Stoks, and J.J. de Swart, Phys. Rev. C **44**, R1258 (1991).
[10] R.A.M. Klomp, V.G.J. Stoks, and J.J. de Swart, Phys. Rev. C **45**, 2023 (1992).
[11] V. Stoks, R. Timmermans, and J.J. de Swart, Phys. Rev. C **47**, 512 (1993).
[12] At the time we first started to follow this approach, the analysis of the *np* data was still in progress. This is the reason that the model we started with is the Nijm92*pp* potential, rather than the (more obvious) Nijm93 potential.
[13] S. Okubo and R.E. Marshak, Ann. Phys. (NY) **4**, 166 (1958).
[14] R. Bryan and B.L. Scott, Phys. Rev. **177**, 1435 (1969).
[15] T.A. Rijken, R.A.M. Klomp, and J.J. de Swart, Nijmegen Report No. THEF-NYM-91.05 (unpublished).
[16] A.M. Green, Nucl. Phys. **33**, 218 (1962).
[17] M. Aguilar-Benitez *et al.*, Particle Data Group, Phys. Lett. B **239**, 1 (1990).
[18] P.M.M. Maessen, Th.A. Rijken, and J.J. de Swart, Phys. Rev. C **40**, 2226 (1989).
[19] M. Svec, A. de Lesquen, and L. van Rossum, Phys. Rev. D **46**, 949 (1992).
[20] S.D. Protopopescu, M. Alston-Garnjost, A. Barbaro-Galtieri, S.M. Flatté, J.H. Friedman, T.A. Lasinski, G.R. Lynch, M.S. Rabin, and F.T. Solmitz, Phys. Rev. D **7**, 1279 (1973).
[21] There are several misprints in Ref. [4]: in Eq. (6) the second expression should read $\mathcal{V}_2^{(V)} = -\frac{2}{3}\mathbf{k}^2\mathcal{V}_3^{(V)}$; the m^2 in front of $\phi_C^1(r)$ in Eq. (15) should be dropped; the ∇^2 operator in Eq. (16) should operate on S_{12} as well as $[(-\nabla^2)^n\phi_T^0(r)S_{12}]$; similarly, Eq. (19) should have $[(-\nabla^2)^n\phi_{\rm SO}^0(r)\mathbf{L}\cdot\mathbf{S}]$; and the coefficient in front of the Q_{12} operator in Eq. (34) should be divided by 4.
[22] J.R. Bergervoet, P.C. van Campen, R.A.M. Klomp, J.-L. de Kok, T.A. Rijken, V.G.J. Stoks, and J.J. de Swart, Phys. Rev. C **41**, 1435 (1990).
[23] J. Schwinger, Phys. Rev. D **3**, 1967 (1971).
[24] J. Binstock and R.A. Bryan, Phys. Rev. D **4**, 1341 (1971).
[25] J.J. de Swart and M.M. Nagels, Fortschr. Phys. **26**, 215 (1978).
[26] B.D. Day, Phys. Rev. C **24**, 1203 (1981).
[27] J.L. Friar, G.L. Payne, V.G.J. Stoks, and J.J. de Swart, Phys. Lett. B **311**, 4 (1993).
[28] D.C. Zheng and B.R. Barrett, University of Arizona report, 1993.
[29] C. van der Leun and C. Alderliesten, Nucl. Phys. **A380**, 261 (1982).
[30] N.L. Rodning and L.D. Knutson, Phys. Rev. C **41**, 898 (1990).
[31] M.W. Kermode, S. Klarsfeld, D.W.L. Sprung, and J.P. McTavish, J. Phys. G **9**, 57 (1983).
[32] V.G.J. Stoks, P.C. van Campen, W. Spit, and J.J. de Swart, Phys. Rev. Lett. **60**, 1932 (1988).
[33] D.M. Bishop and L.M. Cheung, Phys. Rev. A **20**, 381 (1979).
[34] C.P.F. Terheggen *et al.* (unpublished).
[35] M.H. MacGregor, R.A. Arndt, and R.M. Wright, Phys. Rev. **182**, 1714 (1969).

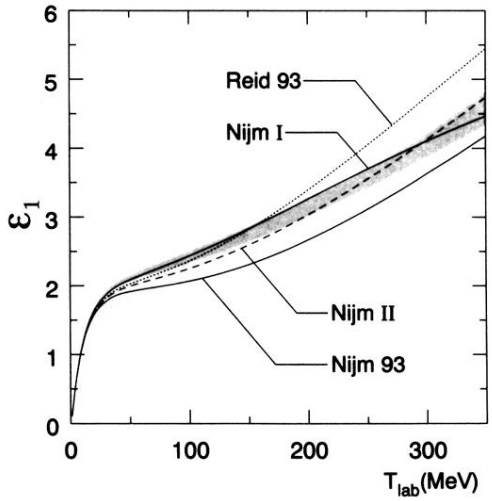

FIG. 1. The mixing parameter ϵ_1 of the various potentials and of the Nijmegen PWA93. The shaded band denotes the statistical error on ϵ_1 as obtained in the Nijmegen partial-wave analysis.